FIFTH AUSTRALASIAN CONFERENCE

on

HYDRAULICS AND FLUID MECHANICS

at

University of Canterbury, Christchurch, New Zealand

1974 December 9 to December 13

DISCHARGE FROM AN AUTOCLAVE SYSTEM

by

W.A. WOODS and D. d. OWEN

SUMMARY

The paper introduces the discharge process as an emergency method of relieving the pressure in an autoclave system. The theoretical aspects of the unsteady flow in the pipework are discussed and consideration is given to the mesh method of calculation for subsonic and supersonic flow. The techniques of treating the moving shock wave and the temperature discontinuity are discussed and the method of starting the calculation is also explained. Next the results of pressure~time calculations are compared with measurements on both a full scale and a model autoclave. The agreement between the results is excellent and this confirms the validity of the theoretical treatment.

W.A. Woods, Mechanical Engineering Dept., University of Liverpool, England.
D. d. Owen, Manor High School, Crosby, Liverpool, England; formerly Mechanical Engineering Dept., University of Liverpool, England.

NOTATION

- a speed of sound
- $\textcircled{a}$ reference speed of sound
- $\hat{a}$ speed of sound after expansion to reference pressure
- C_p specific heat at constant pressure
- C_v specific heat at constant volume
- D pipe diameter
- D_1, D_2 mesh fractions: Figs. 1, 2, 3
- $f = \frac{\tau_w}{\frac{1}{2}\rho u^2}$ friction factor
- f_1, f_2 functions of
- h heat transfer coefficient
- $k = \frac{C_p}{C_v}$ isentropic exponent
- L reference length
- $M = \frac{W}{a_1}$ non-dimensional speed of shock wave, also mesh number: Fig. 4.
- N_{RF} temperature recovery factor
- p pressure
- $\textcircled{p}$ reference pressure
- q rate of heat transfer to gas per unit time per unit mass of gas
- t time
- $\textcircled{T}$ reference temperature
- R gas constant
- u gas velocity
- W speed of shock wave: Fig. 2
- $X = \frac{x}{L}$ non-dimensional distance coordinate
- XP non-dimensional distance moved by shock wave: Fig. 2
- x distance coordinate
- $Z = \frac{\textcircled{a} t}{L}$ non-dimensional time
- $\left.\begin{aligned} \alpha &= \hat{a}/\textcircled{a} \\ \beta &= a/\textcircled{a} - \frac{k-1}{2}\frac{u}{\textcircled{a}} \\ \lambda &= a/\textcircled{a} + \frac{k-1}{2}\frac{u}{\textcircled{a}} \end{aligned}\right\}$ characteristic parameters
- ρ density
- τ_w shear stress at wall
- ψ_j dummy variable

Subscripts

1 denotes low pressure region ahead of shock wave
2 denotes high pressure region between shock wave and contact surface
3 denotes region between contact surface and expansion fan
4 denotes region between expansion fan and autoclave, also initial condition within autoclave

Various letters are used to denote points, see Figs. 1-4

1. INTRODUCTION

In chemical plants, such as those used in the production of tetra-ethyl-lead, the process reactions are carried out in large pressure vessels which are termed autoclaves. In certain circumstances the reaction can become unstable and as the normal regulating procedures are unable to prevent the pressure rising, an emergency situation develops. In these circumstances, a thin metal disc, which seals the autoclave from a large discharge pipe, ruptures at a predetermined pressure. This action causes the contents of the autoclave to discharge rapidly and, thus, major disaster is avoided.

The discharge process occurs in two parts; first, there is a wave action period which is followed by a quasi-steady flow period. A simplified adiabatic and frictionless approach to the discharge problem was described by Woods and Thornton (1)* and the present paper reports further developments in this work. An extension of the mesh method of Benson et al (2) and somewhat similar to (3), which treats subsonic and supersonic flow between moving boundaries, and a technique for commencing the calculation based upon (1) are described. The treatment of a moving shock wave and temperature discontinuity is also given. The resultsof computer calculations are compared with measurements from both full scale and model tests and excellent agreement is found. This confirms the validity of the theoretical work.

2. THEORETICAL ASPECTS

In this section features of the basic unsteady flow are discussed and this is followed by a treatment of the shock wave and temperature discontinuity boundaries. The technique used to commence the mesh calculation is also outlined. The open end boundary and the autoclave boundary are not discussed since they are similar to boundary conditions for engine systems (4). However, steady flow tests on the model autoclave gave an effective area ratio based upon the outlet pipe cross sectional area of 0.7 and this value was used in the calculations for both the model and full scale autoclave systems.

2.1 Basic unsteady flow

The partial differential equations of continuity, momentum and energy for unsteady flow of a perfect gas in a constant area duct are transformed using the method of characteristics to give the following characteristic equations (2), (3), (4), (5)

$$\left(\frac{dX}{dZ}\right)_{\substack{\lambda \\ \beta}} = \frac{u}{\textcircled{a}} \pm \frac{a}{\textcircled{a}} \qquad 1.$$

For the λ and β characteristics

$$\left.\begin{matrix} d\lambda \\ d\beta \end{matrix}\right\} = \left(\frac{\lambda+\beta}{\alpha}\right)\frac{d\alpha}{2} \mp \frac{fL}{D}\frac{(\lambda-\beta)\,|(\lambda-\beta)|}{(k-1)}\left[1 \mp \frac{2(\lambda-\beta)}{(\lambda+\beta)}\right] dZ + \frac{k-1}{(\lambda+\beta)}\frac{qL}{\textcircled{a}^3}\, dZ \qquad 2.$$

* References are given at the end of the paper.

For the path line characteristics $\left(\dfrac{dX}{dZ}\right)_{\alpha} = \dfrac{u}{@}$ - - - - - - - - - - - - - - - 3.

$$d\alpha = \frac{2(k-1)}{(\lambda+\beta)^2}\,\alpha\left[\frac{qL}{@^3} + \frac{2fL}{D}\left|\left(\frac{\lambda-\beta}{k-1}\right)^3\right|\right]dZ \text{ - - - - - - - - 4.}$$

where $\lambda = \dfrac{a}{@} + \dfrac{k-1}{2}\dfrac{u}{@}$, $\beta = \dfrac{a}{@} - \dfrac{k-1}{2}\dfrac{u}{@}$ and $\alpha = \dfrac{\hat{a}}{@}$

These equations are solved numerically using a mesh method somewhat similar to (2), as illustrated by Fig. 1. This illustrates an extension to the method for supersonic flow.

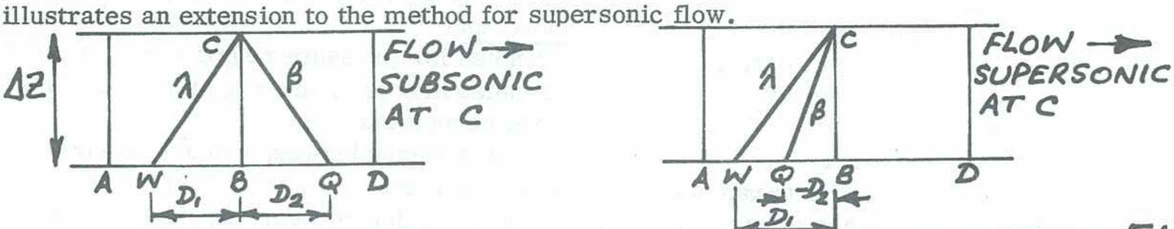

MESH METHOD FOR SUBSONIC AND SUPERSONIC FLOW FIG.1

The friction factor $f = \dfrac{\tau_W}{\frac{1}{2}\rho u^2}$ has been found to have values of 0.003 and 0.005 for the full scale and the model autoclave systems respectively. The heat transfer term is evaluated using the Reynold's Analogy in the form $\dfrac{h}{\rho|u|C_p} = f/2$. The temperature of the pipe wall is assumed to be the same as the initial temperature of the gas in the pipe and also equal to the initial temperature of the autoclave contents. This temperature is selected as the reference temperature (T). Accordingly the reference speed of sound is $@ = \sqrt{kR(T)}$. The heat transfer rate becomes

$$q = \frac{2f|u|}{(k-1)D}\,@^2\left[1 - \left(\frac{a}{@}\right)^2 - N_{RF}\left\{\frac{k-1}{2}\left(\frac{u}{@}\right)^2\right\}\right] \text{ - - - - - - - - - 5.}$$

where N_{RF} is the recovery factor. A value of 0.9 has been found to be a reasonable choice for steady flow from (5) and this has been used for the internal mesh points of the calculations.

The general method of calculation for the internal mesh points follows similar lines to that described in (2) (3) & (4) but the moving boundaries are described next.

2.2 Moving shock wave boundary

The shock wave in the present work moves into stationary gas and the following equations apply to this case (5)(6). It should be noticed that in this sub-section (2.2) the unsubscripted symbols apply to the condition at the shock wave on the high pressure side.

$$p/p_1 = p/(p) = \frac{1}{k+1}\left(2kM^2 - k + 1\right) \text{ - - - - - - - - - - - - 6.}$$

this may be rearranged to give

$$\alpha = \frac{\hat{a}}{@} = \frac{a/@}{\left[\frac{1}{k+1}\left(2kM^2 - k + 1\right)\right]^{\frac{k-1}{2k}}} = \frac{\frac{\lambda+\beta}{2}}{\left[\frac{1}{k+1}\left(2kM^2 - k + 1\right)\right]^{\frac{k-1}{2k}}} \text{ - - - - 7.}$$

The equation for the gas velocity on the high pressure side of the shock wave is,

$$\frac{u}{a_1} = \frac{u}{@} = \frac{2}{k+1}\left(M - \frac{1}{M}\right) = \frac{\lambda-\beta}{(k-1)} \text{ - - - - - - - - - - - - - - - 8.}$$

The Rankine-Hugoniot relationship may be expressed as,

$$\left(\frac{\lambda+\beta}{2}\right) = \frac{a}{a_1} = \frac{a}{@} = \left\{\frac{p/p_1\left[1 + \left(\frac{k-1}{k+1}\right)\frac{p}{p_1}\right]}{p/p_1 + \left(\frac{k-1}{k+1}\right)}\right\}^{\frac{1}{2}} \text{ - - - - - 9.}$$

Now it may be shown from equations 6, 8 and 9 that λ is a unique function of M, thus:-

$$\lambda = \left[\left\{\frac{(2kM^2-k+1)\left[1+\frac{(k-1)(2kM^2-k+1)}{(k+1)^2}\right]}{2kM^2}\right\}^{\frac{1}{2}} + \left(\frac{k-1}{k+1}\right)\left(M-\frac{1}{M}\right)\right] \text{---} 10.$$

for brevity we may write

$$\lambda = f_1(M)$$

Now the λ value can also be expressed using the characteristic equation of state. For the purpose of this evaluation, subscripts, which correspond to Fig. 2, are added for clarity. Thus,

$$\lambda_F = \lambda_W + \delta\lambda_{WF} \text{ --------------------------- } 11.$$

The term $\delta\lambda_{WF}$ is evaluated using a finite difference form of the upper part of equation 2.

Values of λ_W, β_W and α_W are found by linear interpolation, using

$$\psi_W = \psi_C + D_1(\psi_C - \psi_G) \quad (\psi = \lambda, \beta, \alpha) \text{ -------- } 12.$$

where,

$$D_1 = \frac{(k+1)\lambda_C - (3-k)\beta_C - 2(k-1)\frac{XP}{\Delta Z}}{\frac{2(k-1)}{\Delta Z} + (k+1)(\lambda_C - \lambda_G) - (3-k)(\beta_C - \beta_G)} \text{ -------------- } 13.$$

and mean speed of the shock wave over the time step is used,

$$XP/\Delta Z = \left(\frac{M_F + M_C}{2}\right) \text{ ------------------------ } 14.$$

Now the set of equations 11, 12, 13 and 14 may, in principle, be regarded as

$$\lambda_F = f_2(M_F) \text{ ------------------------ } 15.$$

In order to solve the shock wave boundary problem we need to find a value for $M = M_F$ which satisfies equations 10 and 15. This may be expressed as a single equation, as follows:-

$$f_1(M_F) - f_2(M_F) = 0 \text{ ---------------- } 16.$$

A numerical method using a hyperbolic interpolation technique is used to find the solution.

Having discussed the shock wave boundary, the temperature discontinuity boundary is considered next.

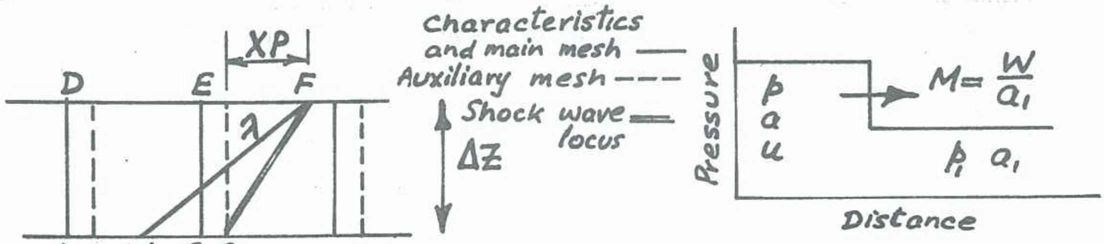

SHOCK WAVE BOUNDARY FIG. 2

2.3 Moving temperature discontinuity

The temperature discontinuity is a somewhat similar problem to that of the shock wave but in place of the shock wave equations there is the equality of pressure and velocity across it. In this case the calculation is direct and, with reference to Fig. 3, values of λ, β and α are known at the beginning of the time step at points R-1, R, R+1 etc. The values at the auxilliary mesh points A, D and G are found by linear interpolation using equations such as

$$\lambda_A = \lambda_{R-1} + (\lambda_R - \lambda_{R-1})\Delta X \text{ ---------------------- } 17.$$

The distance moved by the temperature discontinuity is ΔD and it is found from

$$\Delta D = \left(\frac{\lambda_L - \beta_L}{k-1}\right)\Delta Z \text{ -------------------------- } 18.$$

The distance D_1 is determined from,

$$D_1 = \frac{(k+1)\lambda_L - (3-k)\beta_L - \frac{2\Delta D}{\Delta Z}(k-1)}{\frac{2(k-1)}{\Delta Z} + (k+1)(\lambda_L - \lambda_A) - (3-k)(\beta_L - \beta_A)} \text{ --------- } 19.$$

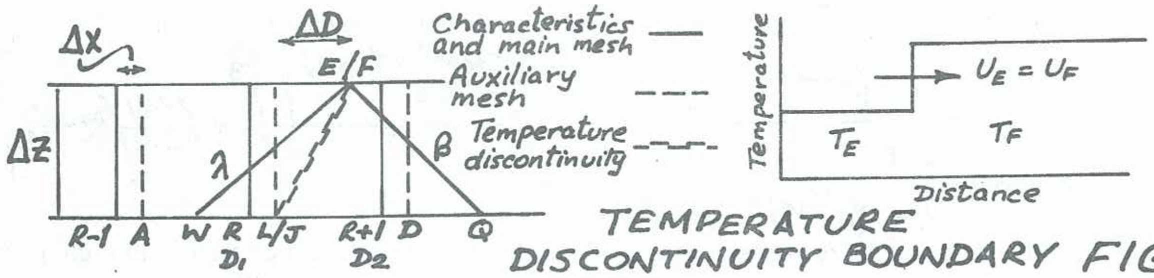

TEMPERATURE DISCONTINUITY BOUNDARY FIG.3

and the property values at W are found by linear interpolation using:-

$$\psi_W = \psi_L - D_1(\psi_L - \psi_A) \quad (\psi = \lambda, \beta, \alpha) \text{ - - - - - - - - - - - - - - } 20.$$

A path line calculation is used to calculate α_E from

$$\frac{\alpha_E - \alpha_L}{\alpha_L} = \frac{4fL}{D}\frac{|(\lambda_L - \beta_L)|}{(k-1)(\lambda_c + \beta_L)^2}\left[1 - \left(\frac{\lambda_L + \beta_L}{2}\right)^2 + \frac{(\lambda_L - \beta_L)^2}{k-1}\right]\Delta Z \text{ - - - - - - } 21.$$

The value of λ_E is found using

$$\lambda_E = \lambda_W + \delta\lambda_{WE} \text{ - - - - - - - - - - - - - - } 22.$$

where $\delta\lambda_E$ is found using a finite difference version of equation 2.

The calculation of the β characteristic is dependent upon whether the temperature discontinuity crosses a mesh or not. Fig. 3 shows the case where the mesh is not crossed; only this case is described here. In this situation,

$$D_2 = \frac{(k-3)(2\lambda_D - \lambda_G) + (k+1)(2\beta_D - \beta_G) + \dfrac{2(k-1)\Delta D}{\Delta Z}}{\dfrac{2(k-1)}{\Delta Z} - (k-3)(\lambda_G - \lambda_D) - (k+1)(\beta_G - \beta_D)} \text{ - - - - - - - - - - } 23.$$

and, again, linear interpolation equations are used,

$$\psi_Q = \psi_D + (D_2 - 1)(\psi_G - \psi_D) \quad (\psi = \lambda, \beta, \alpha) \text{ - - - - - - - - - - } 24.$$

The path line equation 4 is applied to find α_F, in a similar manner to the way equation 21 was used to find α_E.

Next, the lower part of equation 2 is applied to QF to $\delta\beta_{QF}$ from which

$$\beta_F = \beta_Q + \delta\beta_{QF} \text{ - - - - - - - - - - - - - - - - } 25.$$

Hence, from the above equation the following parameters have been determined - $\alpha_E, \lambda_E, \alpha_F$ and β_F and it remains to calculate β_E and λ_F.

The conditions of equality of pressure and velocity across the contact surface lead to the following relationships:-

$$\beta_E = \frac{2\beta_F\alpha_E + \lambda_E(\alpha_E - \alpha_F)}{(\alpha_F + \alpha_E)} \text{ - - - - - - - - - - - - } 26.$$

and

$$\lambda_F = \frac{2\lambda_E\alpha_F + \beta_F(\alpha_F - \alpha_E)}{(\alpha_E + \alpha_F)} \text{ - - - - - - - - - - - - } 27.$$

Hence, conditions across the temperature discontinuity at the end of the time step are determined.

In the next section the singularity condition at the beginning of the calculation is discussed.

2.4 Starting problem

Prior to bursting the diaphragm, the gas at a high pressure region 4 is separated from that at atmospheric pressure region 1 and both gases are at rest. Following rupture of the disc an unsteady gas motion is initiated within the pipe, as shown in Fig. 4, and the object of the starting procedure is to provide the initial data for the mesh calculation. This is necessary because the commencement of discharge is a singularity problem identical to that in a shock tube. An initial time step is used during which frictionless adiabatic flow is assumed to occur. The duration of the time step shown in Fig. 4 is the minimum period needed to locate: (i) at least three mesh points between the shock wave and the contact surface, (ii) at least two mesh points in region 3, between the expansion fan and the contact surface, and (iii) at least three mesh

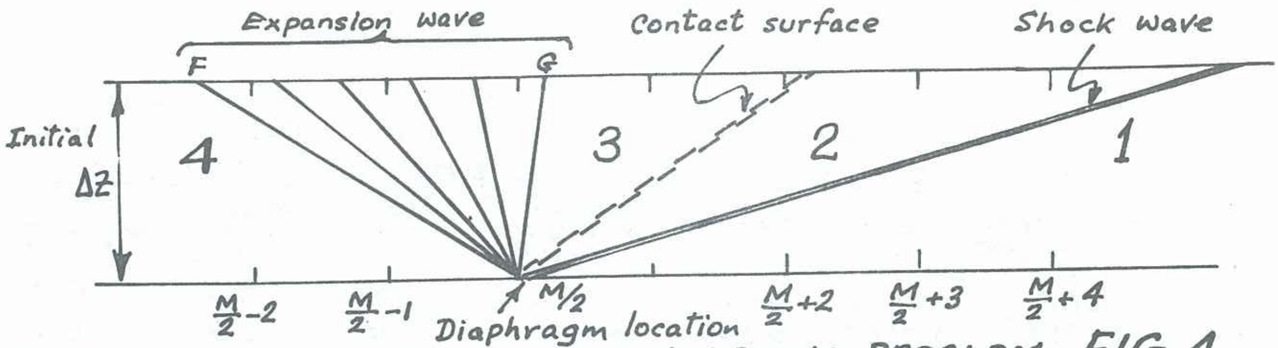

POSITION DIAGRAM FOR THE STARTING PROBLEM FIG. 4

points within the expansion wave (F-G) in Fig. 4. The basic problem is the determination of the two intermediate gas dynamic states in regions 2 and 3. The requirements about the number of mesh points within each region are controlled by the needs of the moving shock wave, the contact surface and interpolation within the expansion fan.

The calculation is direct and the non-dimensional speed of the shock wave M is given (1) by the equation,

$$\frac{p_4}{p_1} = \left(\frac{k-1}{k+1}\right)\left[\left(\frac{2k}{k-1}\right)M^2 - 1\right]\left(1 - \frac{(k-1)(M^2-1)}{(k+1)\left(\frac{a_4}{a_1}\right)M}\right)^{-\left(\frac{2k}{k-1}\right)} \quad \text{-------} \quad 28.$$

The velocity behind the shock wave is given by equation 8, and equations 6 and 9 may be used to show that

$$\frac{a_2}{a_1} = \left\{1 + \frac{2(k-1)}{(k+1)^2}\left[kM^2 - \frac{1}{M^2} - (k-1)\right]\right\}^{1/2} = \frac{\lambda_2 + \beta_2}{2} \quad \text{-----} \quad 29.$$

Further, equation 6 may be used with equation 29 and the definition of α to give,

$$\alpha_2 = \frac{\left\{1 + \frac{2(k-1)}{(k+1)^2}\left[kM^2 - \frac{1}{M^2} - (k-1)\right]\right\}^{1/2}}{\left[1 + \frac{2k}{k+1}\left(M^2 - 1\right)\right]^{\frac{k-1}{2k}}} \quad \text{------------} \quad 30.$$

In region 3 the conditions are found from the following relations.

Prior to discharge, $a_4 = a_1 = @$, and across the contact surface $p_3 = p_2$ and $u_3 = u_2$, hence:-

$$\lambda_2 - \beta_2 = \lambda_3 - \beta_3 \quad \text{-----------------------} \quad 31.$$

and

$$\frac{\lambda_2 + \beta_2}{\alpha_2} = \frac{\lambda_3 + \beta_3}{\alpha_3} \quad \text{-----------------------} \quad 32.$$

The change of state through the expansion fan is assumed to be isentropic and this gives,

$$\frac{a_3}{@} = \left(\frac{p_2/p_1}{p_4/p_1}\right)^{\frac{k-1}{2k}} = \frac{\lambda_3 + \beta_3}{2} \quad \text{------------------} \quad 33.$$

and, also,

$$\alpha_3 = \alpha_4 = 1\Big/\left(p_4/p_1\right)^{\frac{k-1}{2k}} \quad \text{------------------} \quad 34.$$

The conditions within the expansion fan are found by linear interpolation between points F and G on Fig. 4. The horizontal distances of F and G from the bursting diaphragm are ΔX_F and ΔX_G where

$$\Delta x_j = \left[\frac{3-k}{2(k-1)}\lambda_j - \frac{k+1}{2(k-1)}\beta_j\right] \quad (j = F, G) \quad \text{--------} \quad 35.$$

Hence, the main new features of the theoretical treatment have been discussed and these were used, together with other better known techniques (2), (4), (5), to prepare a computer program which calculated the whole discharge process. The results of calculations performed with this computer program are compared with experiments, in the following section.

3. COMPARISON WITH EXPERIMENTS

Experiments were carried out on both a full scale and a model autoclave. The general configuration of each is shown on the inset of Fig. 6 and the relevant dimensions are given in Table I and on the inset on Fig.8.

TABLE I : DETAILS OF AUTOCLAVES AND DATA USED IN CALCULATIONS

Dimension or factor	Autoclave Vol. excluding pipe m^3	Pipe dia m	Pipe length m	Location of bursting disc m from A: Fig6	Friction factor f	Temperature recovery factor N_{RF}	Effective area ratio for autoclave outlet
Full scale	2.288	0.2032	9.144	4.572	0.003	0.9	0.75
Model	0.0355	0.0508	9.144	4.572	0.005	0.9	0.75

Preliminary calculations were performed using mesh numbers of 20, 40, 100 and 250. It was found that 100 meshes was a suitable number to use. Calculations were also performed using various friction factors, from frictionless adiabatic flow f=0 up to a value of f=0.005. From the results friction factors of f=0.003 & f=0.005 were selected for calculations on the full scale and model autoclaves respectively. The effect of friction factor is to prolong the period of discharge and also increase the maximum pressure and the general level of pressure in the discharge pipe.

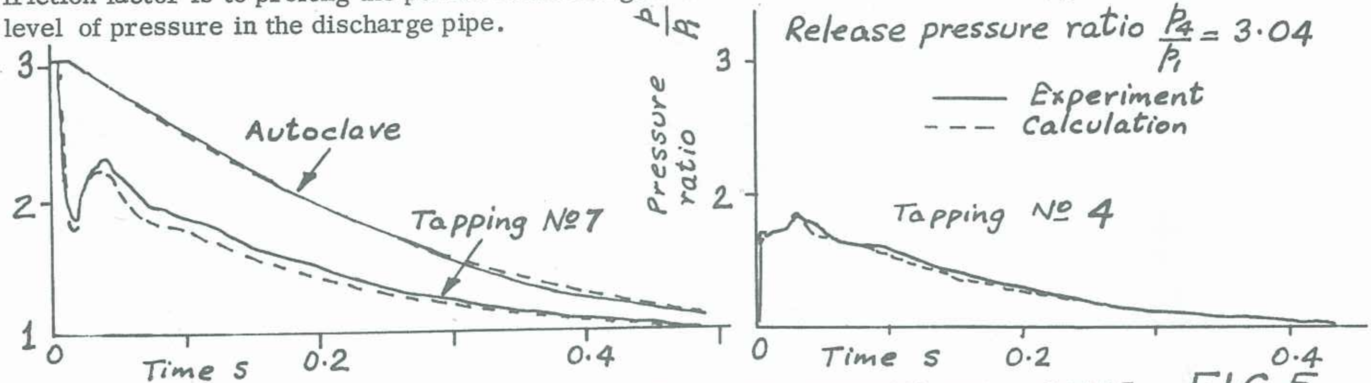

COMPARISON BETWEEN EXPERIMENT AND THEORY: FULL-SCALE FIG.5

The comparison with the full scale test is shown in Fig. 5 for a low release pressure ratio p_4/p_1=3.04 and in Fig. 6 for a high release pressure ratio p_4/p_1=7.12. The results show very good agreement between the calculated and experimental results. The data used in the calculations is shown in Table I.

Comparisons with the model tests are shown in Figs. 7 & 8 for release pressure ratios p_4/p_1 = 7.12 and p_4/p_1 = 21.4 respectively. The agreement is once again very good. In the model tests at the higher

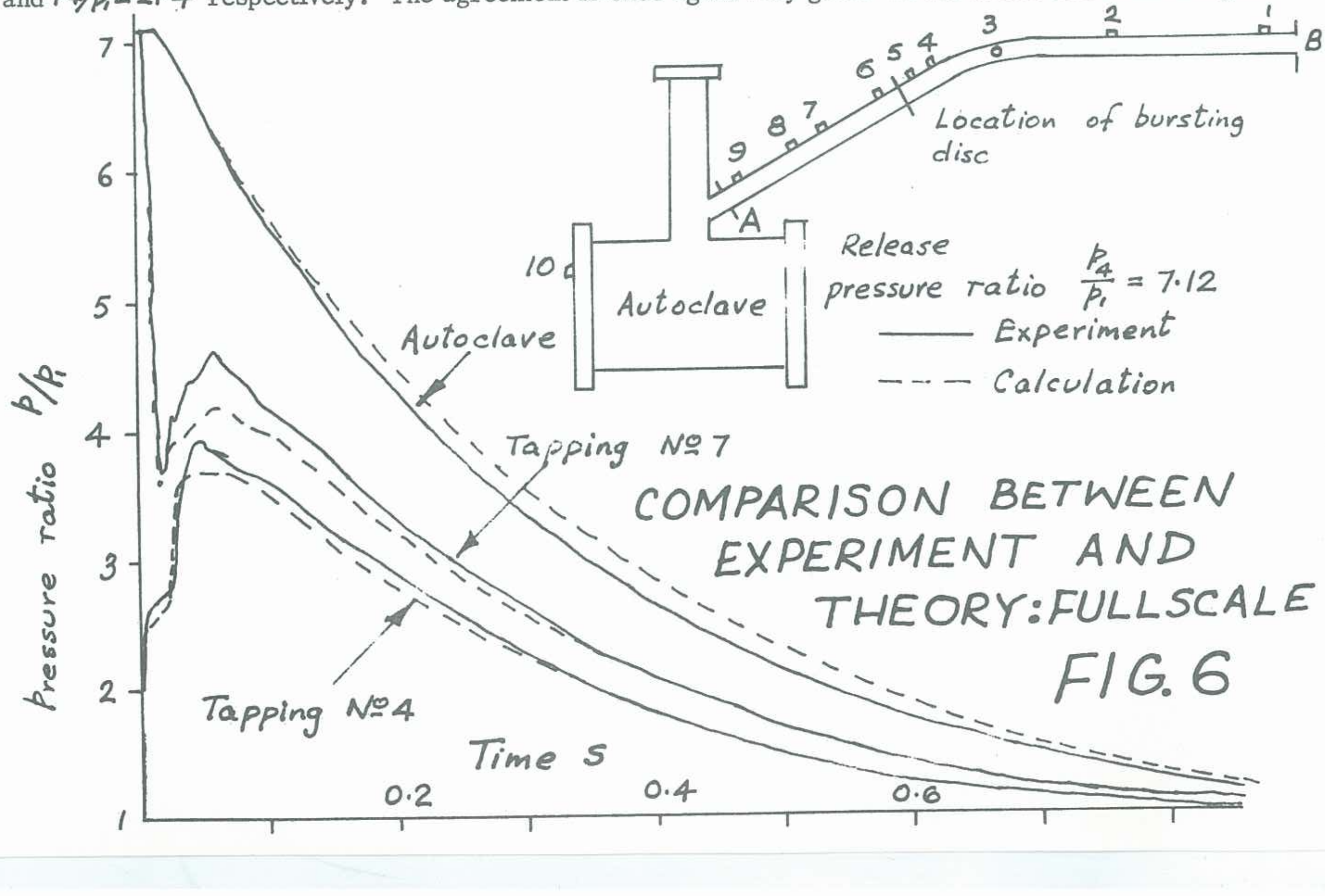

COMPARISON BETWEEN EXPERIMENT AND THEORY: FULLSCALE FIG. 6

release pressures supersonic flows occur in the discharge pipe. The data for these calculations is shown in Table I. The results of the comparisons confirm the validity of the theoretical method.

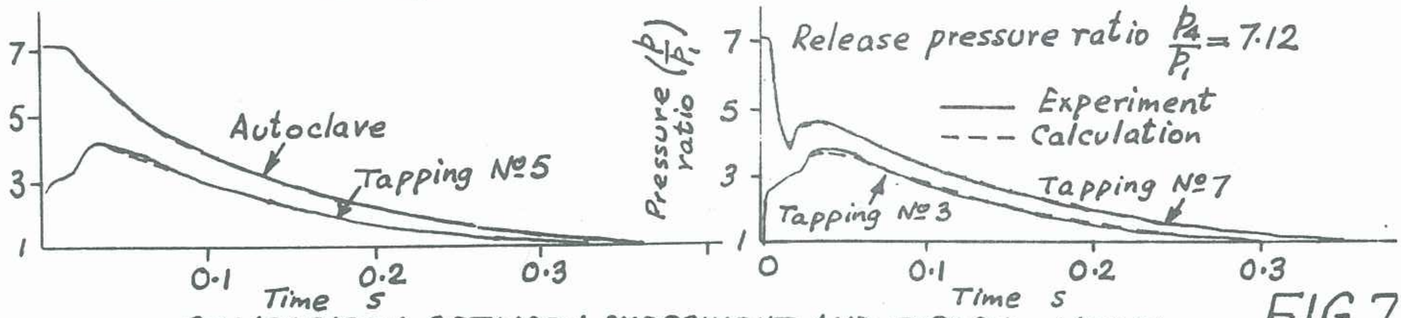

COMPARISON BETWEEN EXPERIMENT AND THEORY: MODEL FIG 7

4. CONCLUDING REMARKS

A comprehensive theoretical treatment of calculating discharge from an autoclave and pipework system has been developed.

The theoretical method has been validated for both subsonic and supersonic flows by comparing test results and calculations. Comparisons between calculations and tests on full scale and model autoclave systems have shown excellent agreement.

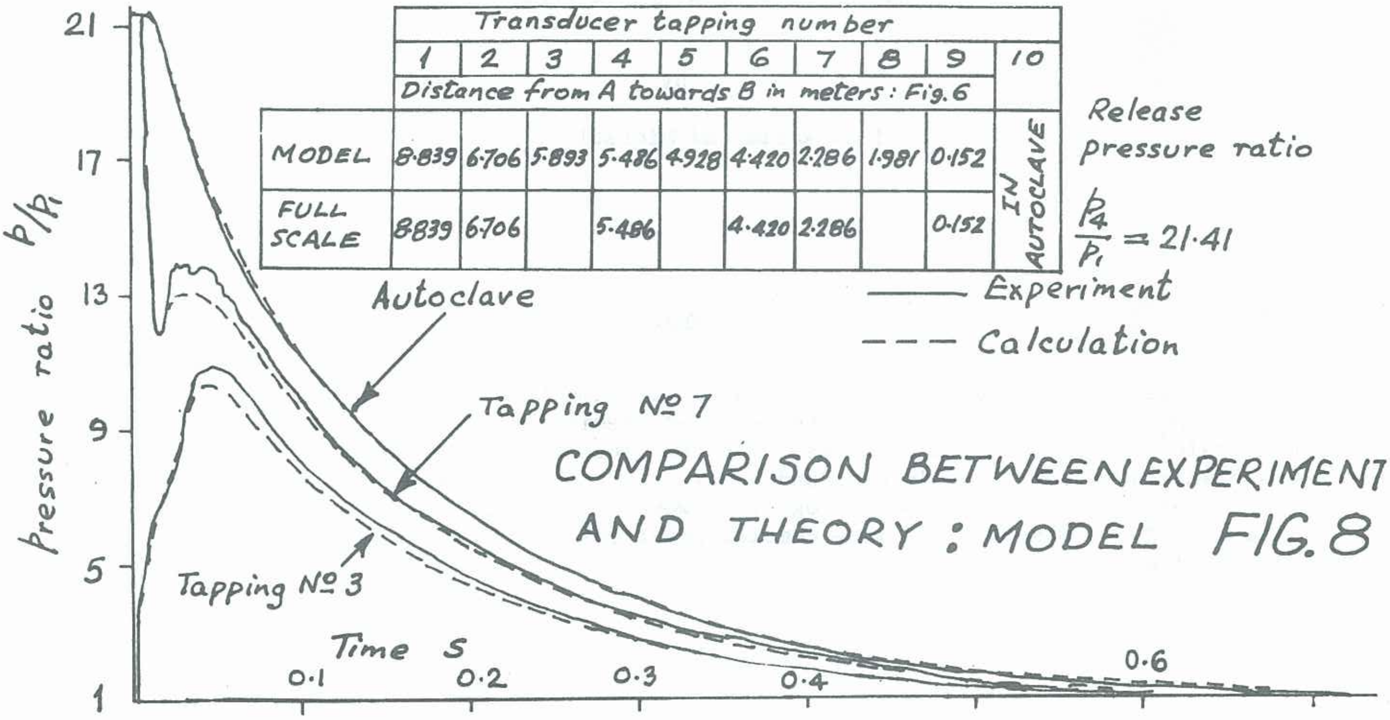

	Transducer tapping number									
	1	2	3	4	5	6	7	8	9	10
	Distance from A towards B in meters: Fig.6									
MODEL	8.839	6.706	5.893	5.486	4.928	4.420	2.286	1.981	0.152	IN AUTOCLAVE
FULL SCALE	8.839	6.706		5.486		4.420	2.286		0.152	

COMPARISON BETWEEN EXPERIMENT AND THEORY : MODEL FIG. 8

5. ACKNOWLEDGEMENTS

The authors wish to acknowledge the help received from Professor J.F. Norbury, the support from the Science Research Council and the Associated Octel Co., and the award of a Research Studentship to D. Owen by the University of Liverpool.

6. REFERENCES

1. Woods, W.A. & Thornton, R.E. — Symp. Ser. No.25, 1968. Instn. Chem. Engrs., London, p.86
2. Benson, R.S., Garg, R.D. & Woollatt, D. — Int.J.Mech.Sci., Vol.6, p.117, 1964.
3. Benson, R.S. — Int.J.Mech.Sci., Vol.14, p.635, 1972.
4. Woods, W.A. & Khan, S.R. — Proc.I.Mech., Vol.182, Pt.3H 1967-68, p.137.
5. Shapiro, A.H. — "Compressible Fluid Flow" Vol.II, The Ronald Press, N.Y., 1954.
6. Friedman, M.P. — J.F.M., 1961, Vol.11, pt.1, p.1.